Computational fluid dynamics analysis on natural convective heating of bottled liquid food during pasteurization

effect of container orientation

Año
2019

Autores
Lespinard, Alejandro Rafael; Badín, Emiliano Emanuel; Santos, María V. y Mascheroni, Rodolfo H.

CITA SUGERIDA
Lespinard, A. R., Badin E. E., Santos M. V. y Mascheroni, R. H. (2019*).* *Computational fluid dynamics analysis on natural convective heating of bottled liquid food during pasteurization: effect of container orientation* . J Food Process Eng. 2019;e12995.

https://doi.org/10.1111/jfpe.12995

Received: 29 June 2018 | Revised: 12 October 2018 | Accepted: 23 December 2018
DOI: 10.1111/jfpe.12995

WILEY Journal of Food Process Engineering

ORIGINAL ARTICLE

Computational fluid dynamics analysis on natural convective heating of bottled liquid food during pasteurization: Effect of container orientation

Alejandro R. Lespinard[1] | Emiliano E. Badin[1] | María V. Santos[2,3] | Rodolfo H. Mascheroni[2,3]

[1]Centro de Investigaciones y Transferencia (CIT Villa María), CONICET - Instituto de Ciencias Básicas y Aplicadas, Universidad Nacional de Villa María, Córdoba, Argentina

[2]Centro de Investigación y Desarrollo en Criotecnología de Alimentos (CIDCA), CONICET La Plata - Universidad Nacional de La Plata, Buenos Aires, Argentina

[3]Depto. de Ingeniería Química, Facultad de Ingeniería, Universidad Nacional de La Plata, Buenos Aires, Argentina

Correspondence
Alejandro R. Lespinard, Campus Universitario. Av. Arturo Jauretche 1555. Villa María (C.P.5900), Córdoba, Argentina.
Email: alespinard@conicet.gov.ar

Funding information
Consejo Nacional de Investigaciones Científicas y Técnicas; Universidad Nacional de La Plata; Universidad Nacional de Villa María; Universidad Nacional de La Plata

Abstract

The aim of this work was to determine natural convective heat transfer rates in bottled liquid food pasteurized using different container orientations; conventional vertical, inverted vertical, and horizontal bottle positions. For this purpose, a computational fluid dynamic (CFD) model was applied to predict the temperature distribution, flow pattern, and quality changes in non-Newtonian fluid foods for three orientations. The numerically predicted temperatures were successfully validated against experimental data and the model allowed to identify the critical point during the thermal process. Results showed that the fluid flow developed in a horizontal orientation provided a better mixing of liquid food and, hence, a more rapid heating of the slowest heating zone compared to a vertical position. Moreover, the horizontal orientation achieved a 47.2% reduction of processing time and quality losses decreased (45.5–46.4%) with respect to a vertical position. These results suggest that a horizontal position could be considered as an interesting alternative for food processors since processing times can be reduced improving the final quality of the product.

Practical Applications

Pasteurization is a heat treatment process applied to a food product with the purpose of destroying disease-producing microorganisms, inactivating spoilage-causing enzymes, and reducing spoilage microorganisms. Overcooking causes detrimental effects in terms of the final product quality. Therefore, providing an adequate process with a desired sterility is one of the challenges to canning industry. In this work, we investigate how to improve, through container orientation modification, the natural convective heat transfer rates during pasteurization of fluid food. These results were obtained by the numerical simulation of the thermal process using CFD analysis which allowed to determine the temperature history and velocity field in the bottled liquid food. From the numerical results, the set of operating conditions that enhance the quality and the safety of the final product was determined, thus minimizing expensive and time-consuming pilot test-runs.

1 | INTRODUCTION

Pasteurization is a heat treatment process applied to a food product with the purpose of destroying pathogenic (disease-producing) microorganisms, inactivating spoilage-causing enzymes, and reducing spoilage microorganisms (Buckenhskes, Gierschner, & Hammes, 1988). Industrial-scale production of pasteurized foodstuffs should ensure the prolongation of the food lifetime while maintaining the sensory, nutritional, and overall quality characteristics of the product (Ghani, Farid, & Chen, 2002). The consumer-led demand for safe and nutritious food products requires a better understanding of the processes involved during production. (Augusto & Cristianini, 2011). When liquid foods are submitted to a thermal process the knowledge of the heat transfer properties, the slowest heating zone (SHZ) location, and the sterilization value distribution throughout the whole system is of paramount importance since these parameters define the efficiency and safety of the process (Pornchaloempong, Balaban, Chau, & Teixeira, 2003). The region in a container that receives the lowest heat transfer, ergo reaching the lowest sterilization treatment during the thermal process is defined as the SHZ (Zechman & Pflug, 1989). The heat transfer of liquid food in a container during pasteurization is carried out under a natural convection condition. To determine the SHZ, complex mathematical equations that represent the combined natural convection and non-isothermal flow of the fluid must be solved to find the velocity profiles and temperature distribution (Kumar, Bhattacharya, & Blaylock, 1990). Measurement of the SHZ is a difficult task since this region is constantly changing its position in spatial coordinates and varies as time elapses (Ghani et al., 2002), also the presence of thermocouples wires alters the free movement of the liquid (Stoforos & Merson, 1990). Therefore, computational fluid dynamics (CFD) is an attractive alternative for engineers and food scientist since it can predict the fluid-dynamic behavior and temperature distribution of the liquid by numerically solving the Navier–Stokes and heat conduction equations. The numerical simulations of non-isothermal flow using CFD can optimize the design of industrial processing equipment since it minimizes the trial-and-error experiments used in the plant (Chhanwal, Anishaparvin, Indrani, Raghavarao, & Anandharamakrishnan, 2010; Kuriakose & Anandharamakrishnan, 2010; Martins, 2006). The use of this technique allows for thermal process evaluation through isothermal and convective current velocity profiles, the localization of cold spot or SHZ, and transformations in the foods such as the inactivation and destruction of microorganisms, enzymes, and nutrients (Augusto, Pinheiro, & Cristianini, 2010). The characteristic of the fluid flow in a container during heating depends on the geometry of the container and its spatial orientation, and small variations can result in substantial differences in processing times (Brandon, Gardner, Huling, & Staack, 1984). With regard to container orientation, it has been found to be an important parameter in heat transfer studies because this phenomenon is different in vertical and horizontal cans due to differences in aspect ratio (Boz & Erdogdu, 2013; Kannan & Sandaka, 2008). It has been reported in the literature that longer heights in vertical cans generate an increase in the heat transfer rate since there is an enhancement of the natural convection condition (Farid & Ghani, 2004; Ghani et al., 2002). On the contrary, Dhayal, Chhanwal, and Anandharamakrishnan (2013) reported the opposite effect using CFD simulations with experimental measurements in horizontal and vertical canned milk; the horizontal placement showed a better heat transfer performance than a vertical configuration. They have employed a container with a lower height-to-diameter ratio and a fluid of lower viscosity than that used by Ghani et al. (2002) and Farid and Ghani (2004), which could explain the different results found by them. Augusto et al. (2010) did not find differences on the evolution of sterilization value (*F*) between conventional, inverted, and horizontal orientations of cans, during beer pasteurization. These authors conclude that lack of differences between the configurations of the cans can be attributed to the fact that beer has less consistency than other food liquids and the fluid convection currents homogenize the temperature distribution. Recently, Dimou, Stoforos, and Yanniotis (2014) studied the effect of particle orientation (peach halves) in liquid particulate cans placed horizontally and vertically, as a result they found that the horizontal cans exhibited a faster heating rate. Another important factor that influences the liquid flow and heat transfer during natural convection in packaged liquid foods is the container geometry. Varma and Kannan (2005) reported the effect of the container geometry (full cone, truncated cone, and full cylinder) and orientation (ranging from 0° to 180°) on the surface heat transfer coefficient in canned foods; the minimum sterilization times were found for the vertically oriented upright full conical configuration followed by a truncate cone and finally the last in performance was the cylinder geometry. When the cylinder was positioned horizontally, it reached a lower sterilization time versus vertical orientation; this was in concordance with results reported by Dhayal et al. (2013).

Most of these previous works have developed models where food viscosity is assumed to behave as that of a Newtonian fluid, containers resistance to the heat penetration is considered negligible and geometries of containers are approximate to regular domains. Thermal processing studies have mostly focused on processing of foods packaged in cans or plastic containers and continuous aseptic processing (without containers). Research studies concerning food processing in glass containers are scarce in the literature (Maroulis & Saravacos, 2003). In glass containers, a headspace is required in order to generate vacuum during the process, this issue has not been previously considered by computational studies. For example, when simulating cans, they were assumed to be fully filled (Erdogdu & Tutar, 2011). However, this is not the case in reality and it is generally expected that headspace might modify the rate of heat transfer in natural convection scenarios. Therefore, literature still lacks a CFD model that evaluates the effect of orientation on pasteurization of partially filled (with headspace) glass bottle with a non-Newtonian fluid food.

The objective of the present work is to apply CFD to obtain an improved quantitative understanding of the effect of container orientation on temperature distribution, flow pattern, position of SHZ, processing time, and quality changes during the pasteurization of a glass bottle containing a non-Newtonian liquid food taking into account the headspace of the container.

2 | MATERIALS AND METHODS

2.1 | Details of system and container geometry

The pasteurization of food packed in a glass bottle can be described as a thermal process where a viscous liquid is heated by immersion in water at boiling temperature (T_{sat} = 100 °C, P_{sat} = 1 atm). The heat transfer during this thermal treatment is governed by a natural convection mechanism. The simulation domain is represented by a commercial glass bottle of tomato puree with 0.275 m in height and an external outer radius of 0.040 m, which contains the liquid food and a headspace. An actual image and geometrical structure of bottle showing the different subdomains are depicted in Figure 1a,b, respectively. The simulation domains were built from the image of the actual geometry of the packaging. This image was digitally processed to obtain a binary file using the Processing Toolbox, MATLAB 6.5 (Math-Works, Natick, Massachusetts), following the steps reported in Santos and Lespinard (2011).

The bottle and liquid food can be assimilated as an axial symmetric two-dimensional domain and the three-dimensional domain was obtained by revolution of the two-dimensional irregular shape. The process was evaluated considering the container with three different orientations: conventional vertical, inverted vertical, and horizontal. In

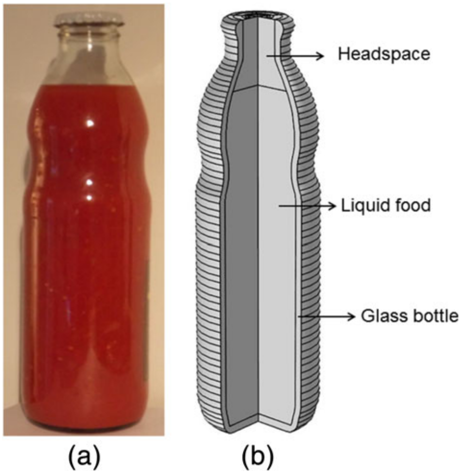

FIGURE 1 Commercial glass bottle of tomato puree: (a) digital photograph and (b) 3D geometry showing the different parts

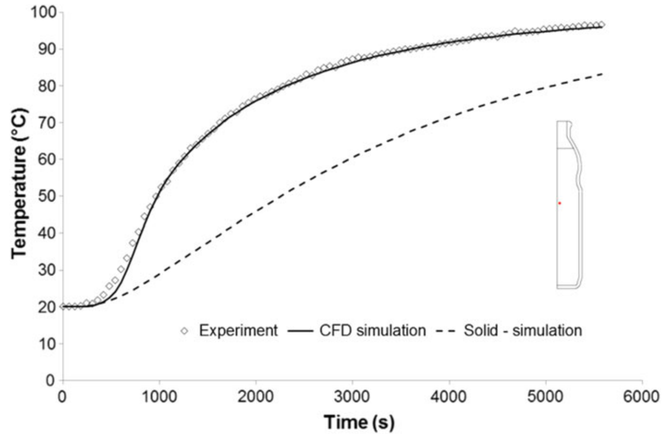

FIGURE 3 Domain and mesh used for the simulation model of horizontal position

the vertical orientations (conventional and inverted), due to the axial symmetry of the container, 2D axisymmetric domains were considered in elaborating the models (Figure 2a,b). For bottle lying horizontally, a 3D analysis must be applied (Figure 3). Symmetry in the longitudinal plane was assumed for horizontal position, reducing the domain to only one half of it.

The models were constructed considering three main materials (glass bottle, liquid food, and headspace) and their thermophysical properties are described in Table 1.

Food materials generally do not follow the Newtonian rheological model, therefore a representative fluid model such as sodium carboxymethyl cellulose (CMC) has been often applied to simulate the rheological behavior of a liquid food during thermal processing (Augusto & Cristianini, 2010, 2011; Farid & Ghani, 2004; Ghani et al., 2002; Ghani, Farid, Chen, & Richards, 1999; Kumar & Bhattacharya, 1991; Lespinard & Mascheroni, 2012; Varma & Kannan, 2005, 2006). A 0.85% w/w CMC was selected since its rheological behavior corresponds to a pseudoplastic fluid and CMC solutions have the advantage that their thermophysical and rheological properties lie in the range common food materials. Moreover, Steffe, Mohamed, and Ford (1986) has recommended this model for tomato puree, carrot puree, green bean puree, apple-sauce, apricot, and banana purees, which are regularly canned and preserved by heating.

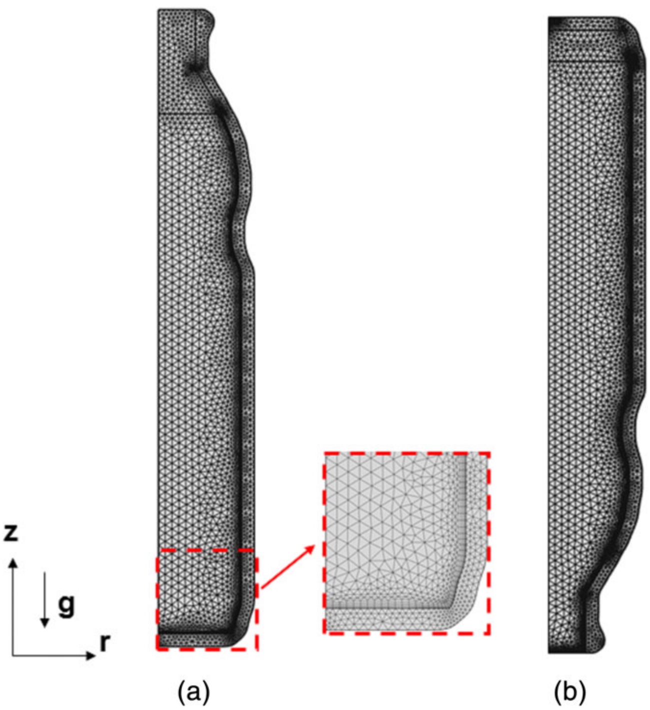

FIGURE 2 Domains and meshes used for the simulation models. (a) Conventional vertical (a zoom of the dotted area is shown) and (b) inverted vertical

2.1.1 | Viscosity model

The viscosity model selected is given by Christiansen and Craig (1962) as

$$\eta = \eta_0 exp\left(\frac{E_0}{RT}\right)\dot{\gamma}^{n-1} \tag{1}$$

where η is apparent viscosity, η_0 is the consistency index, E_0 is the activation energy, R is the universal gas constant (0.00831 kJ/mol/K), T is the temperature and $\dot{\gamma}$ is shear rate, and n is the flow behavior index. For pseudoplastic fluids n is less than one. The values of Equation (1) constants are given in Table 1. The shear rate ($\dot{\gamma}$) is included in the model despite the usual practice of assuming that shear rate anticipated in the natural convection heating is low (zero shear) and thus the viscosity can be assumed to behave as that of a Newtonian fluid (Kumar & Bhattacharya, 1991). However, when the computed shear rate was lower than 0.01/s, the value of η was calculated using a shear rate of 0.01/s.

The headspace was considered as a conductive layer of saturated air, with average properties in the applied temperature range (Augusto et al., 2010; Pinho & Cristianini, 2005; Varga, Oliveira, & Oliveira, 2000). The thickness of the glass container wall in the model was 0.004 m.

2.2 | Mathematical model

2.2.1 | Governing equations

The partial differential equations that govern the non-isothermal flow of a liquid considering natural convection conditions are the mass

TABLE 1 Thermophysical properties used in the simulation model

Material	Property	Value	Source
Liquid food (CMC, 0.85% w/w)	ρ (kg/m^3)	950	Varma and Kannan (2005)
	C_p (J/kg/K)	4,100	
	k (W/m/K)	0.7	
	β (K^{-1})	0.0002	
	η_0 (Pa s^n)	0.002232	
	E_0 (kJ/kg mol)	17.52 10^3	
	n	0.57	
Glass	ρ (kg/m^3)	2,449	Incropera and DeWitt (2002)
	C_p (J/kg/K)	750	
	k (W/m/K)	1.4	
Air	ρ (kg/m^3)	0.361	Pinho and Cristianini (2005)
	C_p (J/kg/K)	1964.95	
	k (W/m/K)	0.023	

(continuity law; Equation (2)), momentum (Newton´s second motion law; Equation (3)), and energy conservation (first Thermodynamics law; Equation (4)).

- The continuity equation or mass conservation law considering an incompressible fluid is

$$\nabla \cdot \mathbf{v} = 0 \tag{2}$$

where $\mathbf{v}$ is the velocity vector and ∇ is the gradient operator.

- The momentum conservation law applying Navier–Stokes Transport equations is

$$\rho \frac{\partial \mathbf{v}}{\partial t} + \rho(\mathbf{v} \cdot \nabla)\mathbf{v} = \nabla \cdot \left[-p\delta + \eta\left(\nabla \mathbf{v} + (\nabla \mathbf{v})^T\right)\right] + F \tag{3}$$

where ρ is density, t is time, p is pressure, δ is Kronecker delta, η is apparent viscosity dependent on temperature and shear rate, and F is the buoyance source.

- Energy conservation equation is

$$\rho c_p \left[\frac{\partial T}{\partial t} + (\mathbf{v} \cdot \nabla)T\right] = k\nabla^2 T \tag{4}$$

where c_p and k are the specific heat capacity and thermal conductivity, respectively.

The Boussinesq approximation was used to describe the natural convection conditions established during pasteurization; it assumes that density remains constant in the governing equations except in the buoyancy term which includes a thermal expansion coefficient β, a local gravitational force and a local temperature difference. The buoyance source (F) is given as follows:

$$F = -\rho_{ref}\beta(T - T_{ref})g \tag{5}$$

where ρ_{ref} and T_{ref} are the density and temperature at the reference condition. According to Ghani et al. (2002), the initial condition was selected as the reference condition.

2.2.2 | Initial and boundary conditions

Initially, the fluid has a uniform initial temperature and no movement; the following initial and boundary conditions were used:

- Uniform initial temperature ($T = T_0 = T_{ref} = 20\ ^\circ$C);
- Velocity of the fluid is null at $t = 0$ in the entire domain ($\mathbf{v} = 0$);
- Velocity of fluid at the packaging walls is null (no slip condition);
- Slip condition was considered at interface air–liquid. The slip condition prescribes a no-penetration condition, $\mathbf{v} \cdot \mathbf{n} = 0$. It implicitly assumes that there are no viscous effects at the interface and hence, no boundary layer develops;
- The boundary condition for the energy equation considers that the external temperature of boiling water is 100 °C and uniform throughout the surface of the container. The resistance to the heat transfer flux at the interface was considered negligible, assuming an infinite coefficient heat transfer. Therefore, constant surface temperature ($T_{outer\ \_\ wall}$) was applied in the simulations at all surfaces of bottle. This implies that the surface temperature reaches the medium temperature (T_{water_bath}) immediately and stays constant throughout the process:

$$\lim_{h \to \infty} \frac{1}{h}(-\mathbf{n}k\nabla T) = (T_{outer\_wall} - T_{water\_bath}) \Rightarrow T_{outer\_wall} = T_{water\_bath} = 100^\circ\mathrm{C}, \tag{6}$$

where $\mathbf{n}$ is the normal outward vector.

Validity of this assumption was shown by Erdogdu, Uyar, and Palazoglu (2010);

- Symmetry boundary conditions on the axis ($r = 0$) and the longitudinal plane (x = 0) were assumed for 2D (vertical positions) and 3D (horizontal position) models, respectively, the equations that represent these conditions are as follows:

$$\mathbf{n} \cdot (-k\nabla T) = 0, \mathbf{v} \cdot \mathbf{n} = 0, \left[-p\delta + \eta\left(\nabla \mathbf{v} + (\nabla \mathbf{v})^T\right)\right] \cdot \mathbf{n} = 0. \tag{7}$$

2.3 | Mesh and time step details

The numerical difficulties encountered during pasteurization of glass containers arise when discretization of the inner fluid in contact with the heated glass walls is carried out, this boundary should be carefully discretized using specific techniques in order to achieve the numerical convergence of the solution (Lespinard & Mascheroni, 2012). The numerical problems occur because temperatures and velocities have their largest variations in this region/boundary. Nonuniform and hybrid grids are useful to circumvent the lack of convergence and to properly resolve the physics of the flow (Rabiey, Flick, & Duquenoy, 2007; Tu, Yeoh, & Liu, 2012). Based on this, quadrilateral mesh along the boundary and triangular mesh structure in the rest of the domain was applied in 2D models (Figure 2a,b), meanwhile a hybrid grid that combines prisms and tetrahedral elements was used in 3D model (Figure 3). Therefore, unstructured meshes with 5,987 and 6,361 elements were developed for conventional and inverted vertical positions, respectively, and a mesh with 265,569 elements was employed to discretize the 3D domain of horizontal position. In all three cases, the use of a finer mesh showed no significant effect on numerical results. The natural convection heating, for conventional vertical orientation, was simulated for 7,000 s. The time step size was automatically adapted by the solver to reach a defined error tolerance. For this purpose, the backward differentiation formula (BDF) time stepping method was used with a relative and an absolute tolerance of 0.01 and 0.001, respectively. It took 100 steps to achieve the first 810 s, another 100 steps to reach 2010 s and 599 steps for the total of 7,000 s of heating. Similar time steps were obtained for the different orientations analyzed in this work.

2.4 | Numerical solution

The nonlinear partial differential equations were numerically solved using the finite element method (FEM). The simulations were carried out in the software Comsol Multiphysics® version 4.0, the BDF was selected as the time-dependent solver and a parallel sparse direct solver (MUMPS) was employed. Lagrange-Quadratic elements were used to discretize the domains. The number of degrees of freedom in the simulation models was 88,882, 96,639, and 3,947,241 for conventional, inverted, and horizontal positions, respectively. For a pasteurization process of 7,000 s, the simulations take about 3.5, 5, and 516 min for conventional, inverted, and horizontal orientations, respectively. The simulation models were run on an Intel Core i5 PC (Windows 7, 3.2 GHz, 8 GB RAM).

2.5 | Model validation

To validate the CFD predictions, experiments were carried out with a bottle in vertical conventional position immersed in a boiling water bath. A temperature recorder (AS-TC, Keithley, Cleveland, Ohio) with Type T—copper-constantan—(Cu-CuNi) thermocouples 0.5 mm thick were used to measure and record the temperature, each 60 s, at a point in the CMC solution with coordinates r = 0.004 and z = 0.14 m (see Figure 4). The thermocouples were inserted in the containers by drilling the metallic lid; after passing the thermocouple a high-temperature resistant seal was used to secure hermeticity around the lid. Experiments were performed in triplicate. The model was validated by comparing numerical predictions with experimental measurements. These comparisons were performed calculating the correlation coefficient (R^2) and the average relative differences (Er_{ave}) (Equation (8)):

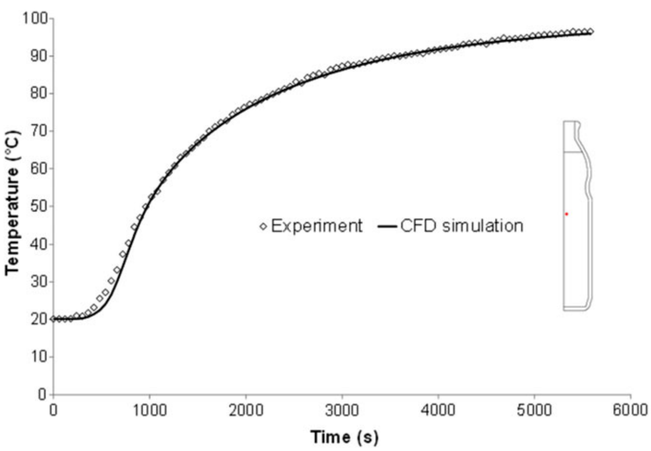

FIGURE 4 Comparison of experimental measurement of temperature, CFD simulation and solid-simulation results at a point of bottle in conventional vertical position. Point location is also shown

$$Er_{ave} = \frac{100}{m}\sum_{i=1}^{m}\frac{|T_s - T_e|}{T_e} \tag{8}$$

where m is the number of experimental points, T_s are predicted temperatures, and T_e are measured temperatures.

2.6 | Determination of the pasteurization times

Pasteurization time was determined on the basis of the critical point (CP) temperature. The CP is the point that corresponds to the coldest point in the liquid food therefore achieving the lowest degree of microbial destruction (i.e., lowest F-value at a given time). The time needed for the CP to reach the cumulative lethality ($F_{93.3}{}^{8.3}$) of 5 min was calculated as recommended for those products of high viscosity and acidity such as tomato puree (Holdsworth, 1997). The cumulative lethality was calculated using Equation (9), as the integral of the lethal rate L along the processing time. The following F-value equation is used to quantify the effects of heat treatment and time with respect to the microorganism inactivation (Holdsworth & Simpson, 2007):

$$F = \int_0^t L dt = \int_0^t 10^{(T-93.3)/8.3} dt \tag{9}$$

2.7 | Quality changes determination

The final quality of the pasteurized product is greatly influenced by the thermal treatment. In order to quantify the effect of a certain thermal treatment on the quality attributes of a foodstuff, equations similar to the F-value are used; in this case by C-value (cooking value) equations. Mansfield (1962) was the first to introduce the concept and it has been extensively applied until present as standard nomenclature for thermal treatments (Holdsworth, 1997). In the present work, to evaluate an average deterioration of quality parameters in the liquid food, the average cooking value (C_{ave}) was determined by numerical integration (Equation (10)), using the simulated temperatures for the food domain (Ω) obtained through the simulation model. A reference temperature (T_{ref}) of 100 °C and a thermal resistance factor (z_c) of 33 °C were considered for estimations. The value of z_c was chosen as the average of those values corresponding to the deterioration kinetics of foods quality parameters (Ohlsson, 1980).

$$C_{ave} = \int_0^t \left(\frac{\int_\Omega 10^{\frac{T(t,\Omega)-T_{ref}}{z_c}} \partial\Omega}{\int_\Omega \partial\Omega} \right) \partial t \tag{10}$$

3 | RESULTS AND DISCUSSION

3.1 | Model validation

Comparison of the experimental temperature measurements and CFD model predictions for the point with r = 0.004 and z = 0.140 m are shown in Figure 4 for the case of the bottle in conventional vertical orientation. Additionally, to analyze the effect of convection on thermal history at the validation point, a predicted temperature profile was obtained by carrying out numerical simulations considering the fluid (CMC solution) as a solid with equal thermophysical properties, data presented in Figure 4. As shown in this figure, the predictions by CFD model were in good agreement with the experimental results. A slight variation in the model predictions and experimental measurements was observed at beginning of the process. This difference can be attributed to the random characteristic of fluid flows at beginning of heating, as well as to the formation of *Bernard Cells*, as described by Augusto and Cristianini (2010). The values obtained for Er_{ave} and R^2 were 1.31% and 0.999, respectively. The simulation model was thus considered successfully validated and afterwards employed for studying the effect of the bottle orientation. The predicted temperatures by CFD model were almost identical to the case of pure conduction heating (solid assumption of CMC in the simulation) until 360 s of process, however as time elapsed (t > 360 s) the convective currents showed a strong influence on the temperature profile which clearly indicates that the conduction mechanism is no longer valid and governing the heat transfer rate.

3.2 | Velocity and temperature profiles

Figures 5a,b and 6 show predicted velocity vectors and temperature profiles for the conventional, inverted, and horizontal orientations, respectively, after 75, 570, 1,005, 1,500, 2010, and 3,000 s of process. The arrows length defines the magnitude of the velocities and arrowheads show their sense. The general behaviour of heat transfer and fluid motion is similar for the three orientations studied. In all cases, temperature profiles show that at the beginning of process (t = 75 s) a conduction mechanism is governing the heat transfer. As

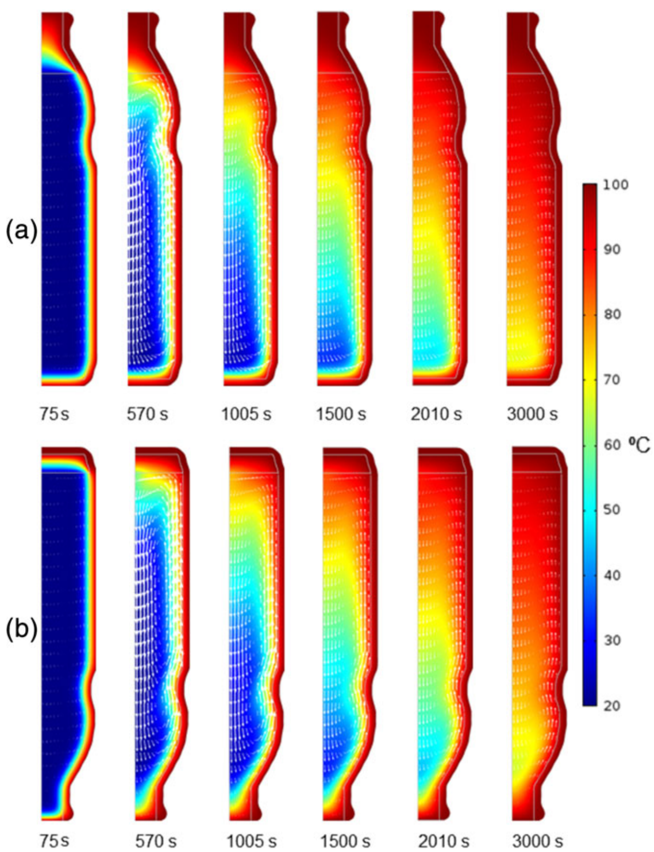

FIGURE 5 Velocity vectors and temperature profiles for (a) conventional and (b) inverted orientations, at different times

time elapses the conduction transitions into a convection heat transfer mechanism. As heating progresses, the mode of heat transfer changes from conduction to convection. This transition occurs because as the liquid near the bottle walls is heated it expands having a lower density compared to the internal liquid which remains at a lower temperature (higher density). The low-density fluid is submitted to an upward buoyancy force moving toward the top of the bottle. This liquid carries colder liquid by viscous drag to the upper sections. When the warm liquid reaches the air–liquid surface it starts moving in radial direction toward the core; the cold liquid due to its higher density moves downwards. As the cold liquid drops to the lower parts of the bottle, it mixes with other cold layers and a new cycle of events starts over generating a recirculating flow. These findings have also been reported by other authors during the thermal processing of in-package liquid foods. A similar flow was also observed by Augusto and Cristianini (2010) in their simulation of the heating of CMC packaged in long neck beer bottle positioned vertically. The recirculation of flow in thick canned foodstuffs was also reported by Ghani et al. (1999). For the bottle in horizontal position, as it is shown in Figure 7, two directions of fluid currents are generated: one transversely and another axially, which increases the fluid mixing effect. Figure 8 show the change in vertical velocities, at mid-height, with time for the three orientations. At initial times, the magnitude of the velocity increases but as the thermal process evolves the velocities decrease. The variation of the velocity as time elapses can be explained in terms of the Grashof number (Gr) (Equation (11)) that represents the ratio of the buoyancy to viscous force. The value of Gr defines the flow regimes that exist during natural convection: laminar, transition, and turbulent.

$$Gr = \frac{g\beta \Delta T {d_c}^3 \rho^2}{\eta^2} \tag{11}$$

where g is acceleration due to gravity (9.806/ms^2), ΔT is the maximum temperature difference, d_c is the characteristic dimension and β, ρ, and η are the thermal expansion coefficient, density and apparent viscosity of fluid, respectively. The high temperature difference between the wall and the core generate an increase in the buoyancy force which later decreases due to the gradual homogenization of the temperature gradients (see Figures 5 and 6). Viscous forces decrease as the temperature increases until reaching a final constant value. Therefore, as the thermal process evolves the temperature gradients decrease, there is a more uniform distribution of temperatures and the buoyancy force is reduced leading to a significant reduction of velocity. Gr was estimated considering the maximum temperature difference and the minimum viscosity in the domain, and a bottle inner radius of 0.036 m was used as characteristic dimensions (d_c) for the three positions. Thereby, the maximum values of Gr obtained were 3.70 (t = 510 s), 3.37 (t = 555 s), and 2.60 (t = 285 s) for conventional, inverted, and horizontal positions, respectively. The low Gr numbers during the entire thermal treatment validate the laminar flow assumption. As can be seen in Figure 8, a similar behaviour was evidenced during the evolution of velocities with time for the three orientations, and their magnitudes were found to be in the order of 10^{-4}–10^{-5}/ms. The velocity vector showed a maximum value in its magnitude after 570 s. However, significant differences in the magnitudes of vertical velocities can be observed between vertical and

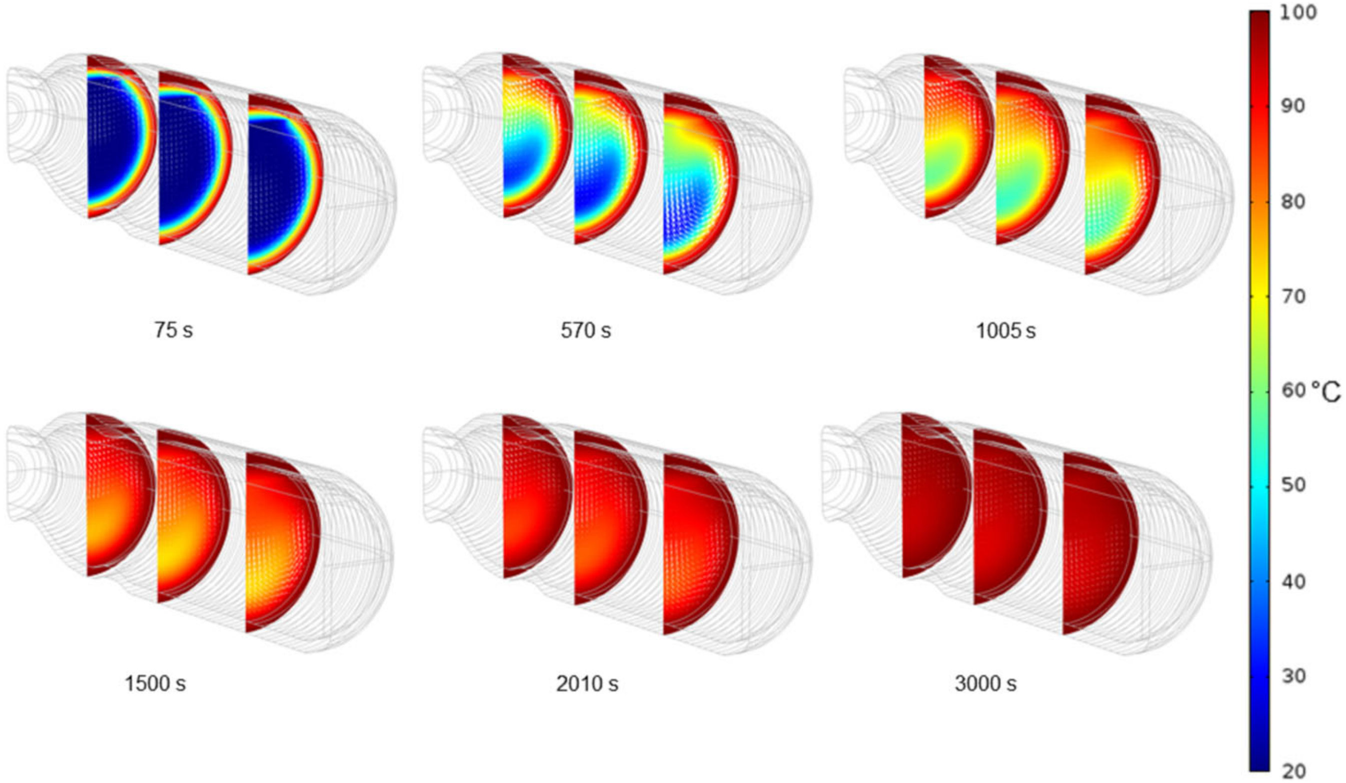

FIGURE 6 Velocity vectors and temperature profiles for horizontal orientation, at different times

horizontal orientations. The results indicate that the vertical velocities developed in the horizontal position were lower than those of vertical orientations, which are in agreement with the values obtained for *Gr*. Maximum values of liquid velocity were obtained near the wall of the container, as expected since in this region there is a maximum temperature gradient. The thickness of the ascending liquid is defined as the distance from the point where the fluid starts to move upward until the radial position of the wall. For all tested orientations (conventional, inverted, and horizontal orientations), this region was approximately 50% of radius of bottle. Kumar and Bhattacharya (1991) and Ghani et al. (1999) reported similar values; 40 and 50%, respectively, for the same liquid packaged in metal can.

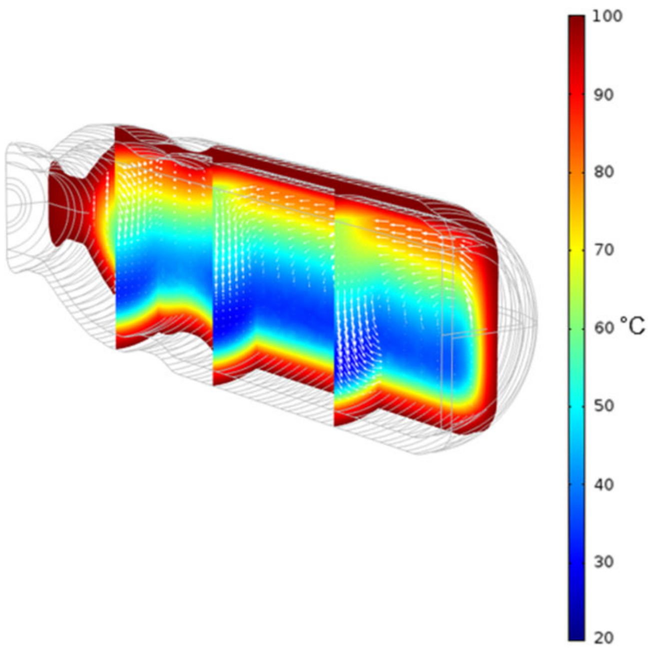

FIGURE 7 Velocity vectors and temperature profiles after 570 s of the thermal process for horizontal position (plans at 25, 50, and 75% of the axial axis and at 25% of the radial axis)

3.3 | SHZ location

The prediction of the time–temperature curve in each node of the discretized domain allowed to calculate the *F*-value versus its position and at a given time. By knowing the *F*-value, the CP was detected as the position that achieved the lowest F-value during the process. This point defines the SHZ and tracking of the CP's movements are shown in Figure 9 for the three orientations. For all orientations, Figure 9 clearly shows that the CP in the bottle (i.e., the location with the lowest cumulative lethality ergo the lowest F-value at a given time) was not at a fixed position in the liquid as it was heated and it varied according to the orientation of the bottle. The heat transfer at the beginning is mainly conductive and the position of the CP was found to be near the geometric center. As the thermal process continues the heat transfer mechanism changes into a convection mode and the CP starts to move in different directions according to the orientation of the bottle. As can be seen in Figure 9a, for conventional vertical orientation, CP moves axially (z direction) downward from beginning of process to 1,470 s and radially (*r* direction) from 1,155 to 1890 s. For the inverted vertical orientation, the CP moves only in an axial direction and, unlike the conventional orientation, there is no radial movement (see Figure 9b). The fact that in the inverted position, the bottleneck is located in the bottom and its thinner shape avoids the

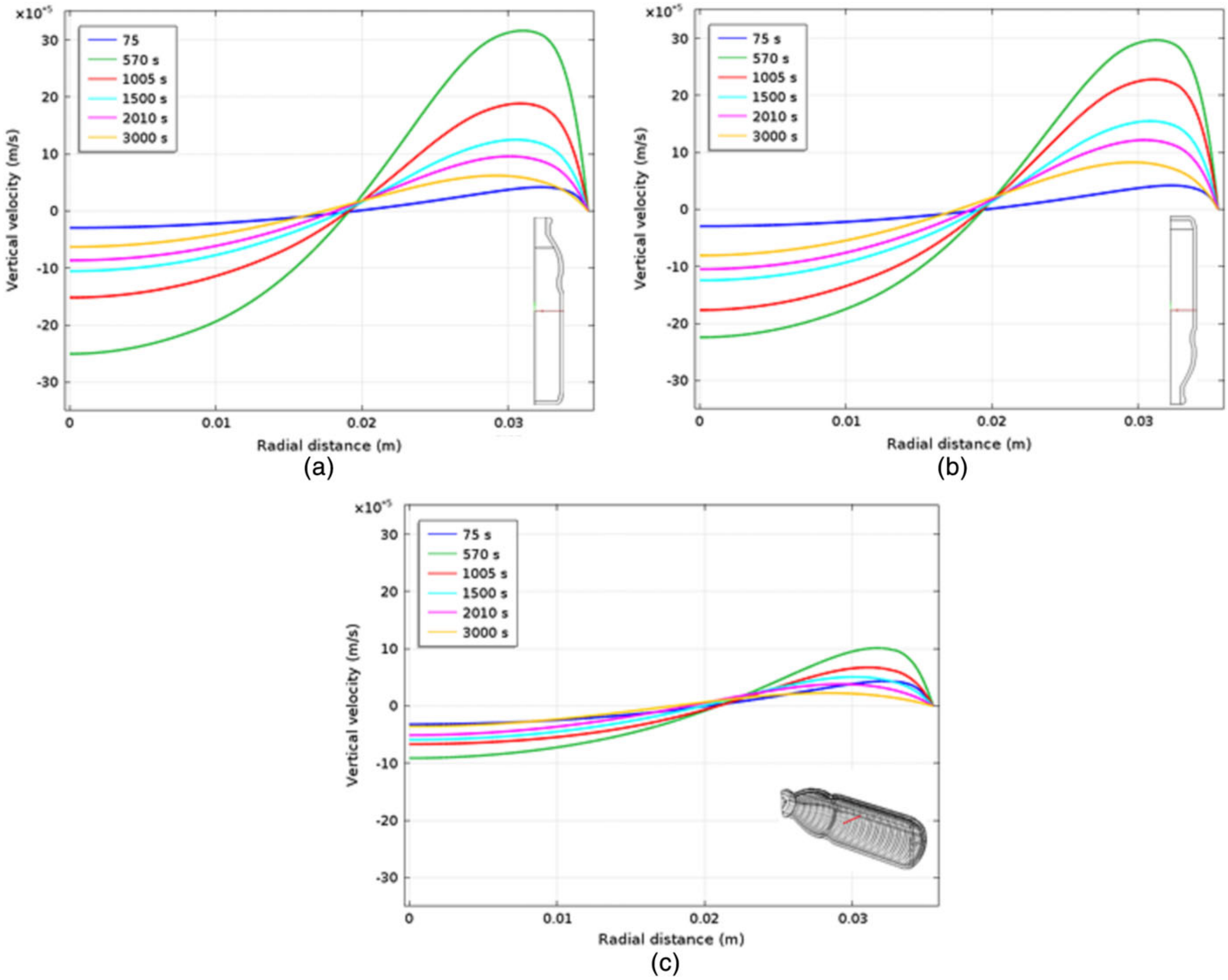

FIGURE 8 Vertical velocity at mid-height vs. radial position for (a) conventional, (b) inverted, and (c) horizontal orientations, at different times

radial movement of CP in this zone may explain this behavior. In this case, vertical movement is developed during 2,100 s from the start of process. For horizontal position, three types of the CP's movements can be possible: vertical (z direction), axial (y direction), and lateral (x direction). From Figure 9c, it can also be observed that the CP moves axially and vertically but not laterally. The CP moves axially during 210 s and then it is settled at a fixed axial position during the rest of process. For its part, the vertical movement is downwards initially, then it remains fixed for a short period of time and finally it starts moving upwards. After a certain period of the thermal process, it is evident from Figure 9 that the CP stops changing its position and settles in a bounded region before it starts to move in the opposite direction. The spatial coordinates of the CP are not equal for the three configurations; the orientation of the bottle influences the movement of the CP during heating. The figure shows that such position is reached after 1,470, 2,100, and 840 s for vertical, inverted, and horizontal positions, respectively. While horizontal position keeps the CP at the same position during shorter period of time than vertical orientations. This difference may be accounted due to the fact that a horizontal orientation heats the fluid more rapidly, therefore the temperature profiles become uniform sooner. When the temperature gradient diminishes, the natural convection transitions into a conduction heat transfer. At this time, the CP starts to move in the opposite direction, which is an indicator of the change of heat transfer mechanism from convective to conductive. Results presented in Figure 9 also indicate that the velocity field influences the movement of CPs; as the velocity decreased in the final stage of the heating process, the CP decreased its movement. Isothermal contours showing the position of SHZ at the end of thermal process are presented in the Figure 10.

3.4 | Pasteurization time and cooking value

The variation of pasteurization time and cooking value with the orientation are compared in Table 2. From Table 2, it is evident that the horizontal orientation is found to be most effective among the three orientations analyzed. The time taken for the CP to reach the accumulated lethality ($F_{93.3}^{8.3}$) of 5 min for horizontal orientation was 47% lower than that of the vertical orientations, whereas no difference was found between conventional and inverted vertical orientations. The rate at which a liquid is heated depends strongly on the fluid-dynamic behavior of the fluid, which is affected by the orientation of the bottle. In horizontal orientations, the two currents (axial and

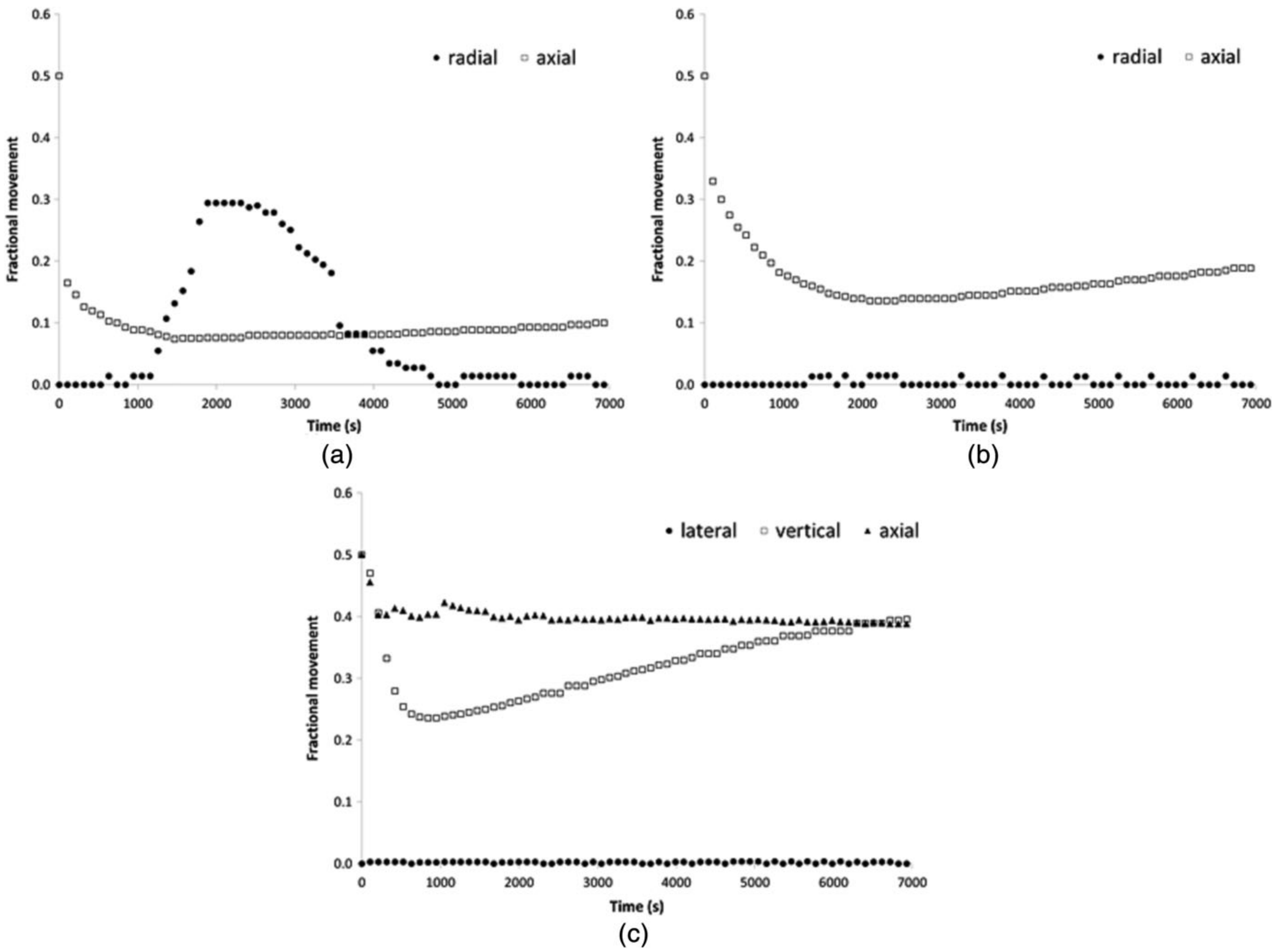

FIGURE 9 Fractional movement of CP for (a) conventional, (b) inverted, and (c) horizontal orientations

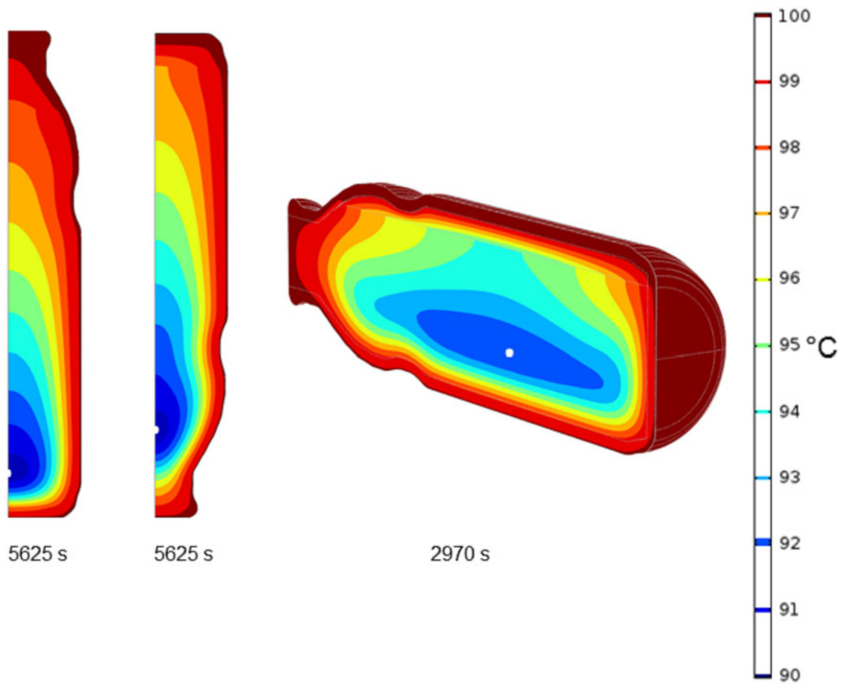

FIGURE 10 Isothermal contours showing the position of the CP (white point) at the end of thermal process for (a) conventional, (b) inverted, and (c) horizontal orientations

TABLE 2 Pasteurization times and cooking values for the different orientations

Orientation	Pasteurization time (s)	Cooking value (C_{ave}) (min)
Conventional	5,625	37.20
Inverted	5,625	36.53
Horizontal	2,970	19.92

transverse) generated in the fluid produce a better mixing effect, which allowed a more rapid heating of the SHZ. This reduction in processing time obtained by horizontal position resulted in a decrease of quality loss around 45.5–46.4%, which was quantified through the average cooking value (C_{ave}). The results obtained in the present work can improve the retention of the nutritional and sensory properties of liquid foods by minimizing the loss of heat-labile food components without compromising the commercial sterility of the product. These results suggest that the horizontal position could be considered as an interesting alternative of processing to conventional vertical position in order to reduce the processing time and improve the quality of liquid food packaged in bottle. Furthermore, minimizing the processing time may lead to lower energy consumption which in turn reduces the final product cost.

4 | CONCLUSIONS

In this study, a CFD model was developed and validated in order to evaluate the effect of container orientation on temperature distribution, flow pattern, SHZ location, processing time, and quality changes in a non-Newtonian fluid food canned in glass bottle during the pasteurization process. The results of this work indicated that among the different orientations, the lowest processing time was obtained for the horizontal orientation, while no difference was found between the process times for the conventional and inverted vertical orientations. Therefore, the lowest loss of quality, quantified by C-value, was achieved when the bottle was horizontally positioned. These results show that the container orientation can contribute to the enhancement of the thermal process without agitation or rotation that would require more energy consumption. The use of CFD has a main advantage which is the ability to determine which set of operating conditions achieve the highest quality with an adequate safety of the final product, without having to run numerous pilot test that are expensive and time-consuming. The numerical predictions obtained in the present work demonstrate that CFD is a powerful tool for engineers and food scientists since it allows to assess the thermal processing of liquids foods submitted to different heating conditions.

ACKNOWLEDGMENTS

Authors acknowledge the financial support of Consejo Nacional de Investigaciones Científicas y Técnicas, Universidad Nacional de La Plata and Universidad Nacional de Villa María from Argentina.

ORCID

Alejandro R. Lespinard https://orcid.org/0000-0001-9466-1771

REFERENCES

Augusto, P. E. D., & Cristianini, M. (2010). Evaluation of geometric symmetry condition in numerical simulations of thermal process of packed liquid food by computational fluid dynamics (CFD). *International Journal of Food Engineering*, *6*, article 1. https://doi.org/10.2202/1556-3758.1695

Augusto, P. E. D., & Cristianini, M. (2011). Numerical simulation of packed liquid food thermal process using computational fluid dynamics (CFD). *International Journal of Food Engineering*, *7*, article 16. https://doi.org/10.2202/1556-3758.2418

Augusto, P. E. D., Pinheiro, T. F., & Cristianini, M. (2010). Using computational fluid-dynamics (CFD) for the evaluation of beer pasteurization: Effect of orientation of cans. *Food Science and Technology (Campinas)*, *30*, 980–986. https://doi.org/10.1590/S0101-20612010000400022

Boz, Z., & Erdogdu, F. (2013). Evaluation of two-dimensional approach for computational modelling of heat and momentum transfer in liquid containing horizontal cans and experimental validation. *Food and Bioproducts Processing*, *91*, 37–45. https://doi.org/10.1016/j.fbp.2012.08.005

Brandon, H., Gardner, R., Huling, J., & Staack, G. (1984). Time-dependent modeling of in-package pasteurization. *Technical Quarterly-Master Brewers Association of the Americas (USA)*, *21*, 153–159.

Buckenhskes, H., Gierschner, K., & Hammes, W. (1988). *Theory and praxis der pasteurization*, 9. Die industrielle Obst-und Gemseverwertung, Braunschweig.

Chhanwal, N., Anishaparvin, A., Indrani, D., Raghavarao, K., & Anandharamakrishnan, C. (2010). Computational fluid dynamics (CFD) modeling of an electrical heating oven for bread-baking process. *Journal of Food Engineering*, *100*, 452–460. https://doi.org/10.1016/j.jfoodeng.2010.04.030

Christiansen, E., & Craig, S. (1962). Heat transfer to pseudoplastic fluids in laminar flow. *AIChE Journal*, *8*, 154–160. https://doi.org/10.1002/aic.690080205

Dhayal, P., Chhanwal, N., & Anandharamakrishnan, C. (2013). Heat transfer analysis of sterilization of canned milk using computational fluid dynamics simulations. *Journal of Food Science and Engineering*, *3*, 571.

Dimou, A., Stoforos, N. G., & Yanniotis, S. (2014). Effect of particle orientation during thermal processing of canned peach halves: A CFD simulation. *Foods*, *3*, 304–317. https://doi.org/10.3390/foods3020304

Erdogdu, F., Uyar, R., & Palazoglu, T. K. (2010). Experimental comparison of natural convection and conduction heat transfer. *Journal of Food Process Engineering*, *33*, 85–100. https://doi.org/10.1111/j.1745-4530.2008.00309.x

Erdogdu, F., & Tutar, M. (2011). Velocity and temperature field characteristic of water and air during natural convection heating in cans. *Journal of Food Science*, *76*, 119–129. https://doi.org/10.1111/j.1750-3841.2010.01913.x

Farid, M., & Ghani, A. A. (2004). A new computational technique for the estimation of sterilization time in canned food. *Chemical Engineering and Processing: Process Intensification*, *43*, 523–531. https://doi.org/10.1016/j.cep.2003.08.007

Ghani, A. A., Farid, M., & Chen, X. (2002). Numerical simulation of transient temperature and velocity profiles in a horizontal can during sterilization using computational fluid dynamics. *Journal of Food Engineering*, *51*, 77–83.

Ghani, A. A., Farid, M., Chen, X., & Richards, P. (1999). Numerical simulation of natural convection heating of canned food by computational fluid dynamics. *Journal of Food Engineering*, *41*, 55–64.

Holdsworth, S. D. (1997). *Thermal processing of packaged foods*. London, England: Chapman Hall.

Holdsworth, S. D., & Simpson, R. (2007). *Thermal processing of packaged foods*. New York, NY: Springer Science & Business Media.

Incropera, F. P., & DeWitt, D. P. (2002). *Fundamentals of Heat and Mass Transfer*. New York, NY: John Wiley & Sons, Inc.

Kannan, A., & Sandaka, P. C. G. (2008). Heat transfer analysis of canned food sterilization in a still retort. *Journal of Food Engineering*, *88*, 213–228. https://doi.org/10.1016/j.jfoodeng.2008.02.007

Kumar, A., Bhattacharya, M., & Blaylock, J. (1990). Numerical simulation of natural convection heating of canned thick viscous liquid food products. *Journal of Food Science*, *55*, 1403–1411. https://doi.org/10.1111/j.1365-2621.1990.tb03946.x

Kumar, A., & Bhattacharya, M. (1991). Transient temperature and velocity profiles in a canned non-Newtonian liquid food during sterilization in a still-cook retort. *International Journal of Heat and Mass Transfer*, *34*, 1083–1096. https://doi.org/10.1016/0017-9310(91)90018-A

Kuriakose, R., & Anandharamakrishnan, C. (2010). Computational fluid dynamics (CFD) applications in spray drying of food products. *Trends in Food Science & Technology*, *21*, 383–398. https://doi.org/10.1016/j.tifs.2010.04.009

Lespinard, A., & Mascheroni, R. H. (2012). Influence of the geometry aspect of jars on the heat transfer and flow pattern during sterilization of liquid foods. *Journal of Food Process Engineering*, *35*, 751–762. https://doi.org/10.1111/j.1745-4530.2010.00624.x

Mansfield, T. (1962). High temperature-short time sterilization. *In Proceedings of the 1st international congress on food science and technology*, 311–316.

Maroulis, Z. B., & Saravacos, G. D. (2003). *Food process design*. New York, NY: Marcel Dekker Co.

Martins, R. (2006). Simple finite volumes and finite elements procedures for food quality and safety simulations. *Journal of Food Engineering*, *73*, 327–338. https://doi.org/10.1016/j.jfoodeng.2005.01.033

Ohlsson, T. (1980). Optimal sterilization temperatures for flat containers. *Journal of Food Science*, *45*, 848–852. https://doi.org/10.1111/j.1365-2621.1980.tb07464.x

Pinho, C., & Cristianini, M. (2005). Three-dimensional mathematical modeling of microbiological destruction of *Bacillus stearothermophilus* in conductive baby food packed in glass container. *International Journal of Food Engineering*, *1*(2). https://doi.org/10.2202/1556-3758.1010

Pornchaloempong, P., Balaban, M., Chau, K., & Teixeira, A. (2003). Numerical simulation of conduction heating in conically shaped bodies. *Journal of Food Process Engineering*, *25*, 539–555. https://doi.org/10.1111/j.1745-4530.2003.tb00650.x

Rabiey, L., Flick, D., & Duquenoy, A. (2007). 3D simulations of heat transfer and liquid flow during sterilisation of large particles in a cylindrical vertical can. *Journal of Food Engineering*, *82*, 409–417. https://doi.org/10.1016/j.jfoodeng.2007.02.011

Santos, M., & Lespinard, A. (2011). Numerical simulation of mushrooms during freezing using the FEM and an enthalpy: Kirchhoff formulation. *Heat and Mass Transfer*, *47*, 1671–1683. https://doi.org/10.1007/s00231-011-0831-7

Steffe, J., Mohamed, I., & Ford, E. (1986). Rheological properties of fluid foods: Data compilation. In M. R. Okos (Ed.), *Physical and chemical properties of food* (pp. 1–13). St Joseph, MI: Am. SOC. Agric. Engrs.

Stoforos, N. G., & Merson, R. L. (1990). Estimating heat transfer coefficients in liquid/particulate canned foods using only liquid temperature data. *Journal of Food Science*, *55*, 478–483. https://doi.org/10.1111/j.1365-2621.1990.tb06791.x

Tu, J., Yeoh, G. H., & Liu, C. (2012). *Computational fluid dynamics: A practical approach* (2nd ed.). Burlington, MA: Elsevier Butterworth-Heinemann.

Varga, S., Oliveira, J. C., & Oliveira, F. A. (2000). Influence of the variability of processing factors on the F-value distribution in batch retorts. *Journal of Food Engineering*, *44*, 155–161. https://doi.org/10.1016/S0260-8774(99)00174-0

Varma, M. N., & Kannan, A. (2005). Enhanced food sterilization through inclination of the container walls and geometry modifications. *International Journal of Heat and Mass Transfer*, *48*, 3753–3762. https://doi.org/10.1016/j.ijheatmasstransfer.2005.03.024

Varma, M. N., & Kannan, A. (2006). CFD studies on natural convective heating of canned food in conical and cylindrical containers. *Journal of Food Engineering*, *77*, 1024–1036. https://doi.org/10.1016/j.jfoodeng.2005.07.035

Zechman, L. G., & Pflug, I. (1989). Location of the slowest heating zone for natural convection heating fluids in metal containers. *Journal of Food Science*, *54*, 205–209. https://doi.org/10.1111/j.1365-2621.1989.tb08602.x

How to cite this article: Lespinard AR, Badin EE, Santos MV, Mascheroni RH. Computational fluid dynamics analysis on natural convective heating of bottled liquid food during pasteurization: Effect of container orientation. *J Food Process Eng*. 2019;e12995. https://doi.org/10.1111/jfpe.12995